The Meteoritical Society

Meteoritics & Planetary Science 57, Nr 9, 1759–1773 (2022)
doi: 10.1111/maps.13900

Composition of the Apollo 17 drive tube 76001 and the nonmare lithologies of the North Massif and Luna 20

Randy L. KOROTEV

Department of Earth and Planetary Sciences and McDonnell Center for the Space Sciences, Washington University, Saint Louis, Missouri 63130, USA
Corresponding author. E-mail: korotev@wustl.edu

(Received 29 March 2022; revision accepted 06 July 2022)

Abstract–Bulk composition data for 24 chemical elements are presented for regolith samples (<1 mm fines) from each of the 62 half-centimeter dissection intervals along the 31 cm length of the 76001 vertical drive tube collected by astronauts at the base of the North Massif at station 6 of the Apollo 17 landing site. The core regolith is nearly uniform in composition with depth although the concentrations of Sc and Sm, for example, decrease from 28.5 μg g^{-1} Sc and 5.93 μg g^{-1} Sm at the top 2.5 cm to 26.9 μg g^{-1} Sc and 5.55 μg g^{-1} Sm at the bottom 2.5 cm. This change reflects an increase with depth in the relative abundance of Sm-poor, feldspathic material, from 48.4% at the top to 50.1% at the bottom. On the basis of compositional mass balance, the feldspathic (nonmare) material of the station 6 regolith requires a substantial proportion of an Mg-rich lithology, ~27% when modeled as troctolite sample 76535. The remaining 73% is nominally Sm-poor anorthositic norite in composition. No such Mg-rich component is required to account for the composition of the regolith of the South Massif (stations 2 and 3). The total feldspathic component of the North Massif regolith, normatively an anorthositic troctolite (74 vol% plagioclase, olivine:pyroxene = 55:45, *Mg′* = 78%), is very similar to that of the nonmare component of the Luna 20 regolith collected 910 km to the southeast on the Crisium ejecta deposit. We also present new composition data for 21, 25, and 16 small lithic fragments (0.1–3.9 mg each) from the regoliths of the Luna 16, 20, and 24 missions.

INTRODUCTION

Astronauts collected regolith cores at six locations in the Taurus–Littrow Valley during the Apollo 17 mission to the Moon. One ("deep drill core," sample numbers 70001–70006) was a rotary drill core 2 cm in diameter that acquired regolith to a depth of 290 cm at a point 200 m west of the lunar module on the valley floor (Laul et al., 1979; Morris et al., 1979; Nagle, 1982). The other five were drive tubes of 4 cm diameter that were pushed or pounded into the regolith. A single drive tube segment was nominally 30 cm long, but the tubes could be concatenated into a double drive tube of 60 cm length (Allton, 1989). Two single drive tubes—(1) tube 70012 at the lunar module on the valley floor and (2) tube 76001 at station 6 on a colluvial deposit at the bottom of the North Massif about 100 m above the valley floor—were collected. Three double drive tubes—(1) tubes 79001/2 at station 9 near Van Serg Crater on the valley floor (Morris et al., 1989; Schwarz, 1987), (2) tubes 74001/2 on the valley floor near Shorty Crater at station 4 (Morris et al., 1978), and (3) tubes 73001/2 on the avalanche deposit ("light mantle") from high on the South Massif at station 3—were obtained.

At this writing, the 73001/2 core is being processed at NASA/Johnson Space Center (JSC) in Houston and analyzed by a variety of techniques (Bell et al., 2022; Elsila et al., 2022; McFadden et al., 2022; Neuman et al., 2022; Shearer et al., 2022; Simon et al., 2022, Sun et al., 2022; Valencia et al., 2022; Valeniciano et al., 2022, Welten et al., 2022; Yen et al., 2022; Zeigler et al., 2022). For comparison, we present here composition data that we obtained in 1992 for the North Massif drive tube 76001 (Table S1 in supporting information). We presented preliminary data in Korotev and Bishop (1993). For comparison to the nonmare components of the station 6 regolith, we also present data and discussion for samples from the Luna 20 regolith on the continuous ejecta deposit of Mare Crisium (Swindle et al., 1991) that we obtained in 1988. We also present new data for samples from Luna 16 and Luna 24.

APOLLO 17, STATION 6

The Apollo lunar module landed in the Taurus–Littrow Valley, an embayment (graben; Hurwitz & Kring, 2016) of Mare Serenitatis bounded by the North and South Massifs. The valley has been flooded with basalt from Mare Serenitatis. The more ancient massifs were, at the time of the mission, assumed to be ejecta deposits or uplifts from the Serenitatis basin impact. Station 6 was located at the interface of the valley floor and the base of the North Massif, which is about 1400 m high above station 6. A mission goal was to collect ancient impact melt from the Serenitatis impact basin for the purpose of establishing the chronology of basin formation. At station 6, astronauts collected samples of impact melt breccia from broken fragments of a boulder that had rolled down the hill from a point 430 m above the valley floor (Schmitt et al., 2017). The 980 m long boulder track was visible from several kilometers away. Later, about half a kilometer to the east, samples from another such boulder were collected at station 7. Extensive discussions of the Apollo 17 site geology are summarized in Muehlberger et al. (1973), Wolfe et al. (1981), Spudis and Ryder (1981), Wilhelms (1987), Spudis et al. (2011), Hurwitz and Kring (2016), and Schmitt et al. (2017).

The 76001 core was collected 10 m southwest and downhill from the station 6 boulder cluster (Nagle, 1979) (Fig. 1) and about 6 m south of the Rover (Schmitt, 2021) on December 13, 1972. The 76001 core is the only Apollo core to have been collected on a slope. During dissection of the core, Nagle (1979) noted that the soil was fine grained but contained an "anomalous" population of large rock fragments, up to 4 cm in longest dimension. Lithic fragments observed during dissection (Nagle, 1979) and in thin section (Papike & Wyszynski, 1980) include mare ("ilmenite") basalt, "crystalline matrix" (impact melt) breccias, "light matrix" (likely also impact melt) breccias, pyroxene–poikilitic melt rocks (likely KREEP-bearing noritic melt breccias), "recrystallized noritic" (granulitic breccias; Stöffler et al., 1980), "dark matrix" (likely regolith) breccias, "ANT" ("anorthositic–noritic–troctolitic rocks"; e.g., Prinz et al., 1973), "orange/black glass" clods, agglutinates,

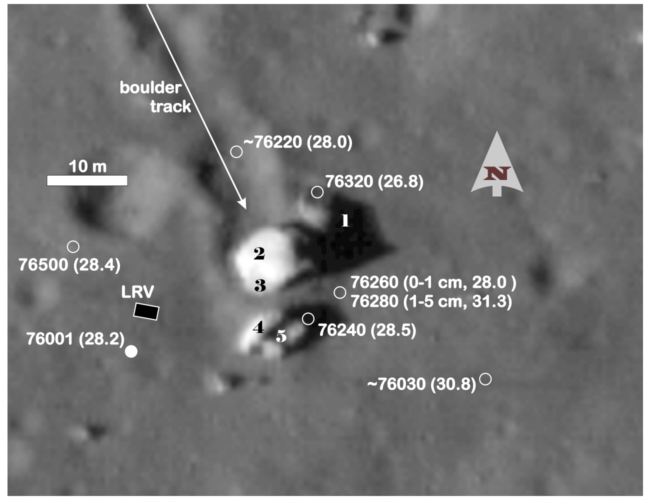

Fig. 1. Location map of regolith samples from station 6, including the track of the station 6 boulder, the five numbered pieces of the fragmented boulder, and the Lunar Roving Vehicle (LRV) (after fig. 6-116 of Muehlberger et al., 1973). The numbers in parentheses are the Sc concentrations (μg g^{-1}) of Figs. 2 and 5. From NAC image M134991788R (NASA/GSFC/Arizona State University). Note that the five-digit sample numbers for surface and trench soils, as collected, end in 0 (zero). After sieving at JSC, the <1 mm sieve fractions end in 1, the 1–2 mm fractions end in 2, and the 2–4 mm fractions end in 3 (e.g., Fig. 3).

individual mineral grains, fragmented vesicular glass, and fragmented glass. Nagle (1979) estimated the ratio of nonmare to mare rocks to be 4:1. He noted that "through most of the core, all equant or tabular particles ... were oriented with the long axis horizontal." KREEP is an acronym for K, REE (rare earth elements), and P that was first applied to a lithologically cryptic, geochemical component that was rich in all incompatible elements and that occurred in a diverse suite of glasses and breccias of noritic composition from the Apollo 12 regolith (Meyer et al., 1971).

Nagle (1979) concluded that "the core had been deposited by slow continuous accumulation [downslope mass wasting], rather than by [in-situ] gardening." He divided the core into six units, largely on the basis of color of the fine-grained material and distribution and size of rock fragments. In thin section, Papike and Wyszynski (1980) observed a major stratigraphic break at ~20 cm depth with the lower unit ("A") richer in clasts of "gabbroic anorthosite" and the upper unit ("B") richer in ilmenite basalt and KREEP-rich noritic breccia. Morris and Lauer (1979) observed that the core regolith (<250 μm grain size fraction) was mature throughout (I_s/FeO >60; Fig. 2), consistent with maturation higher on the slope and accumulation at the bottom. The same conclusion was reached by Fruchter et al. (1980) on the

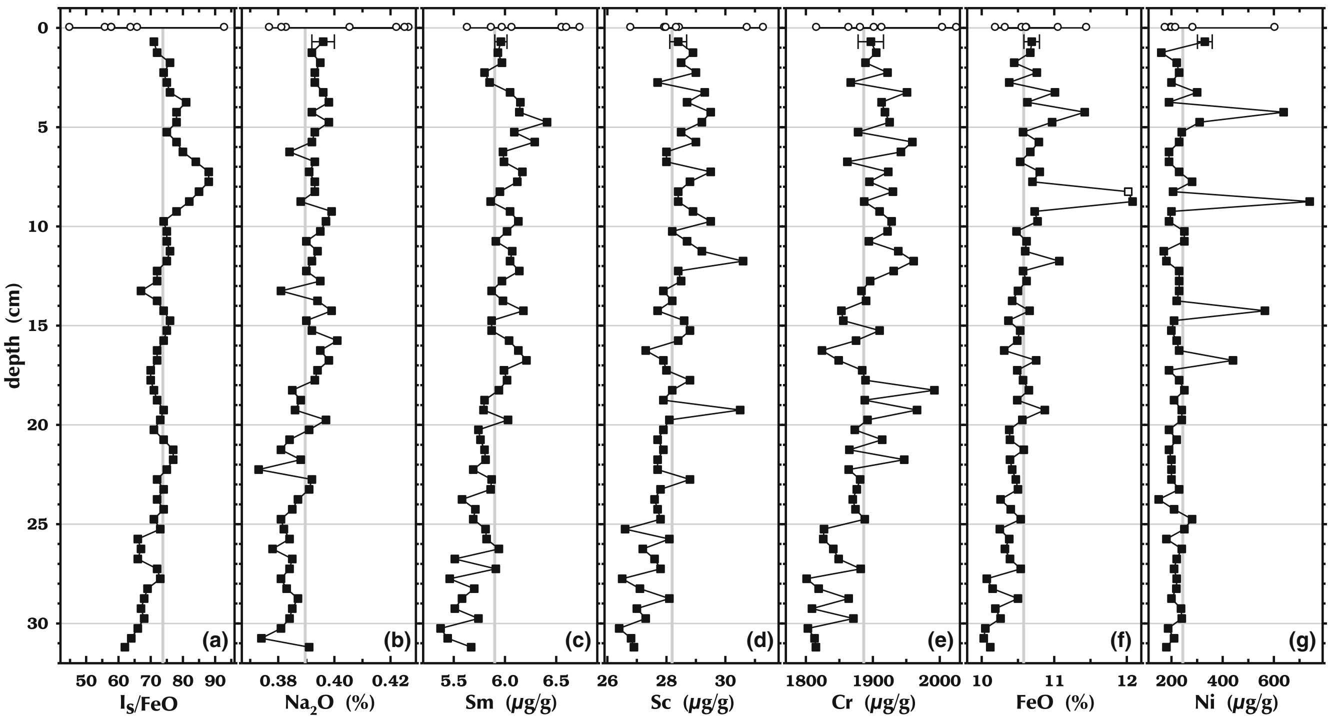

Fig. 2. Variation with depth of (a) I_s/FeO (in <250 µm grain size fraction, three-point running average; Morris & Lauer, 1979) and (b–g) concentrations of six chemical elements in ~0.12 g samples of 76001 (squares). The vertical gray lines represent the core means and the circles at 0 cm represent the seven surface soils from station 6 (Figs. 1 and 5). The error bars at 0.7 cm depth represent typical 1-σ analytical uncertainties. In (a), the high-maturity region at 6–9 cm depth corresponds to stratigraphic unit 5 of Nagle (1979), which is relatively devoid of large lithic fragments. b) Anomalously low-Na samples are likely slightly enriched in olivine (troctolite?). c) High-Sm samples are slightly enriched in nuggets of KREEP-bearing, noritic impact melt breccia (Fig. 3). d, e) Samples with high Sc and Cr contain nuggets of mare basalt (Fig. 3). f, g) Some of the high-Sc samples are also slightly enriched in Fe, but others are rich in Fe because they contain nuggets of FeNi metal. In (f), the unfilled point at 8.25 cm depth represents a sample with anomalously high Co, 238 µg g^{-1} compared to a mean of 34 µg g^{-1} for the rest of the core. However, the sample is not anomalous in Cr, Ni, or Ir, so the anomaly is the result of contamination with terrestrial metal. (Nagle [1979] observed scrape marks on the inside of the drive tube.) Stratigraphic units 3 and 4 (Nagle, 1979; 10.5–22.5 cm depth) are characterized by large lithic fragments. Note that except perhaps for the Sc and Cr anomalies at 12 cm depth, none of the anomalies extend over more than one 0.5 cm dissection level.

basis of cosmogenic radionuclides. Morris and Lauer (1979) noted that FeO concentrations decreased slightly with depth from which they concluded that the highland component increases slightly from the top to the bottom of the core. They estimated, on the basis of their FeO data and the mixing model of Rhodes et al. (1974), that the ratio of highlands to mare material was about 3:1 for the core average.

SAMPLES AND ANALYSIS

We were allocated samples of approximately 120 mg from each of the nominal 0.5 cm dissection intervals along the ~31 cm length of the 76001 drive tube. Samples originated from the first dissection pass (Nagle, 1979) and consisted of sieved <1 mm fines. We obtained composition data for 24 elements by INAA (instrumental neutron activation analysis, Table S1). Analytical procedures were the same as those of Korotev (1991).

In 1987, NASA received from Soviet scientists' 2 g of samples collected on the robotic Luna 16, 20, and 24 missions to the Moon. All the samples are regolith collected with rotary drill cores. At NASA JSC, fragments >0.5 mm in size were sorted into look-alike categories (Taylor, 1987). In 1988 and 1989, we analyzed two samples of <250 µm fines from each mission as well as 21 lithic fragments from Luna 16 (Mare Fecunditatis; Korotev et al., 1988, 1990a), 31 fragments from Luna 20 (highlands between Mare Fecunditatis and Mare Crisium), and 16 fragments from Luna 24 (Mare Crisium; Korotev et al., 1990b). For the Luna 20 samples, we analyzed (1) 14 fragments of nominal "agglutinates and regolith breccias" (sample 22023,7; 0.12–1.00 mg in mass; mean: 0.44 mg), (2) 11 fragments of "feldspathic crystalline" rocks (sample 22023,10; 0.13–0.43 mg in mass; mean: 0.27 mg), and (3) six fragments of "fine-grained crystalline" rocks (sample 22023,3; 0.27–1.54 mg in mass; mean: 0.62 mg). Preliminary data for the first two groups were reported in Korotev and Haskin (1988). Data and analytical procedures for the third group, which we assumed to be impact melt breccias, were reported in Swindle et al. (1991). In Table S2 in supporting information, we present our INAA data for all of the Luna samples.

RESULTS

Station 6 Regolith Composition and Mass-Balance Model

The composition of Apollo 17 regolith samples has been modeled (Table 1) as mixtures of four compositionally distinct suites of components, all of which are represented by lithologies observed petrographically in the regolith. The mixtures include (1) high-Ti mare basalt; (2) pyroclastic orange glass and its black (devitrified) equivalent; (3) KREEP-rich impact melt breccia of noritic composition; and (4) a feldspathic, KREEP-poor component generically identified in older literature as "anorthositic gabbro" (Blanchard et al., 1975; Laul et al., 1981; Rhodes et al., 1974) or "anorthositic norite" (Korotev & Kremser, 1992). The first two components represent the mare, the latter two derive from the highlands massifs. In detail, there are at least four compositionally distinct varieties of high-Ti basalt (Neal & Taylor, 1992) as well as a minor component of VLT (very-low Ti) basalt (Jolliff et al., 1996; Wentworth et al., 1979) in the Apollo 17 regolith. Three compositionally and texturally distinct varieties of noritic, KREEP-bearing, impact melt breccias are known (Jolliff et al., 1996; Spudis & Ryder, 1981) including poikilitic (1.5 ± 0.2% TiO_2, 15 ± 3 $\mu g\ g^{-1}$ Sm, and 1.95 ± 0.20 $\mu g\ g^{-1}$ Eu), aphanitic (0.9 ± 0.3% TiO_2, 13 ± 3 $\mu g\ g^{-1}$ Sm, and 1.4 ± 0.2 $\mu g\ g^{-1}$ Eu), and incompatible trace element (ITE)-rich (1.5 ± 0.3% TiO_2, 23 ± 4 $\mu g\ g^{-1}$ Sm, and 1.95 ± 0.20 $\mu g\ g^{-1}$ Eu). Compositionally, all large samples of mafic impact melt breccia from the North Massif boulders are of the poikilitic variety. Among the 55 lithic fragments of the noritic, KREEP-bearing impact melt breccias from the station 6 regolith studied by Jolliff et al. (1996), none is of the aphanitic composition and 7% ($N = 4$) are of the ITE-rich variety (>18 $\mu g\ g^{-1}$ Sm, Fig. 3); the other 93% are of the poikilitic composition. Not well understood at the time of the early mass-balance ("mixing") models was that the anorthositic component is actually a suite of lithologies that includes ferroan anorthosite, troctolitic anorthosite ($Mg' \approx 87$ = mol% MgO/[MgO + FeO]), ferroan ($Mg' \approx 63$), and magnesian ($Mg' \approx 73$) granulitic breccias of anorthositic norite composition, feldspathic impact melt breccias, and other feldspathic polymict breccias including regolith breccias largely free of mare material (Jolliff et al., 1996).

The highly polymict regolith at station 6 contains subequal proportions of all four major lithologic components but is dominated (~47%) by the feldspathic component (Table 1). Differences in the relative proportions of components predicted among the models of Table 1 result from differences in (1) samples used to represent the station 6 regolith (varies from 1 to 7); (2) sample mass analyzed (the sample of Laul et al. [1981] is very small, 27 mg, compared to that of the other studies' 1400 and 787 g); (3) sets of chemical elements used in modeling (e.g., Rhodes et al. [1974] did not include REEs); and (4) assumptions about the identity and representative composition of the various components. For example, a major compositional distinction between the high-Ti basalt and the orange (picritic) glass is the greater MgO (and Mg') of the orange glass (Fig. 4; Table 1). The model of Laul et al. (1981) predicts a high proportion of orange glass compared to the other models because their anorthositic gabbro component, a composition derived mainly from ferroan granulitic breccias, has a low Mg' (64) compared to that of the other models (68–70) and only the orange glass, among their assumed model components, can supply the missing MgO.

Rhodes et al. (1974) and Korotev and Kremser (1992) noted that the regolith from the North Massif was richer in MgO (Fig. 4) and had higher Mg' than the four-component mass-balance model could account. For example, Rhodes et al. (1974) measured 10.9% MgO in the station 6 soil but the four-component model yielded only 9.4% MgO, an underestimation of 13%. For Laul et al. (1981), their station 6 soil (based on a small sample of 76501) contained 12.0% MgO yet their model only accounts for 8.3% MgO, an underestimation of 30%. Rhodes et al. (1974) suggested "the presence in these soils of small amounts (<5%) of an additional high-magnesian component such as dunite or troctolite." In order to account for the discrepancy Korotev and Kremser (1992) added, somewhat arbitrarily, a mafic (16.8% MgO), high-Mg' (85) component represented by a mixture of 60% troctolite, sample 76535 from the regolith of station 6, and 40% norite, sample 78255 from station 8. Inclusion of this fifth component provided a much better fit to the regolith from station 6. The four-component model underestimated the MgO concentration by 9% whereas the five-component model "overestimated" MgO by 0.2%. Mass balance required 15% of the Mg-rich component (Table 1), a larger fraction than the 5% estimated by Rhodes et al. (1974). Despite these differences in model assumptions and components, the

Table 1. Results of mass-balance models for station 6 surface soils and range of Mg' among model components.

	Mg'	Rhodes et al. (1974)	Laul et al. (1981)	Korotev and Kremser (1992)	This work
Soil Mg'		62.5–65.7	66.5	64.1	62.3–65.7
Mare basalt	45.3–46.3	15.9	9.8 ± 3.5	21.1 ± 0.8	19.9 ± 0.9
Orange glass	53.5–54.9	11.7	17.6 ± 4.1	5.9 ± 0.8	10.8 ± 0.9
Noritic impact melt breccia	69.8–71.1	24.1	18.0 ± 1.3	21.3 ± 0.2	22.1 ± 0.4
Feldspathic	63.7–77.6	48.3	54.8 ± 1.7	50.8 ± 0.5	46.6 ± 0.4
CI chondrite, volatile free				1.2 ± 0.1	0.53 ± 0.05
Σ		100.2	100.2	100.2	100.0*
Feldspathic (anorth. troct.)	77.6	—	—		
Anorthositic norite	69.5	—	—	36.2 ± 1.2	33.9 ± 1.0
Troctolite	87.2	"<5"	—	14.6 ± 1.2	12.7 ± 1.1
Σ mare		27.6	27.4	27.2	30.9
Σ nonmare		72.4	72.8	72.8	69.1

Values in % of component. Results of Rhodes et al. (1974) are based on samples 76241, 76261, 76321, and two samples of 76501 (1400 g total mass). Those of Laul et al. (1981) are for sample 76501 only (28 mg). Those of Korotev and Kremser (1992) and this work are based on all seven samples of Fig. 5 (798 mg total mass). Compositions of model components of this work are presented in Table S3. The models of Korotev and Kremser and this work include a minor (0.5%) component of volatile-free CI chondrite to account for concentrations of Ni, Ir, and Au. Uncertainties are standard deviations.

Anorth. troct. = anorthositic troctolite.

*Constrained to 100.0%.

highlands:mare proportions are similar for all models of Table 1 (2.3:1–2.7:1).

Subsequent to Korotev and Kremser (1992), Jolliff et al. (1992, 1996) studied 395 lithic fragments from 2–4 mm grain size fractions of station 6 soil samples 76280 and 76500 (Figs. 1 and 3). Low-Sm feldspathic lithologies included mainly magnesian granulitic breccias and troctolitic anorthosites. Ferroan anorthosites, ferroan granulitic breccias, and other polymict breccias were less common although regolith breccias and feldspathic agglutinates were frequent.

Based on the observations of Jolliff et al. (1992, 1996), we have revised the model of Korotev and Kremser (1992) for station 6 by experimenting with five feldspathic (not plotted, but 7–14 $\mu g\ g^{-1}$ Sc on Fig. 3), low-Sm (1.0–1.6 $\mu g\ g^{-1}$, Fig. 3) lithologies with a range of Al_2O_3 and Mg' to represent the anorthositic norite component. The lithologies include (1) Apollo 17 ferroan granulitic breccia (Al_2O_3 = 25.8% and Mg' = 63), (2) typical feldspathic lunar meteorites (29.6 and 67), (3) the anorthositic norite component of Korotev and Kremser (1992) (25.5 and 70), (4) high-Mg' lunar meteorite ALHA 81005 (25.8 and 73), and (5) Apollo 17 magnesian granulitic breccia (26.2 and 73). None of the tested anorthositic norite components alone accounts for the high MgO of the station 6 soils (Fig. 4). Thus, we have also tested two mafic lithologies from Apollo 17 as a fifth, Mg-rich component: troctolite sample 76535 (Dymek et al., 1975; Haskin et al., 1974) and dunite sample 72415 (Dymek et al., 1975; Laul & Schmitt, 1975). Mathematically, both Mg-rich components account well for the high MgO of the station 6 soil with any of the five anorthositic norite components. Petrographically, however, the Mg-rich component is cryptic. Samples 72415–72418 (all fragments of one rock), the only rock-sized dunite at Apollo 17, is from the South Massif and Jolliff et al. (1996) did not encounter any olivine fragments among the 395 2–4 mm lithic fragments that they studied from the North Massif. Jolliff et al. (1992, 1996) also did not encounter any troctolites as mafic as sample 76535 although there were numerous highly feldspathic troctolitic anorthosites. The latter, however, do not contain enough MgO to account for the high MgO of the soil (Fig. 4). Likewise, Blanchard et al. (1975) did not observe any mafic, olivine-rich fragments among the 41 1–2 mm lithic fragments (sample 76502) in their study, although they found one feldspathic pink-spinel troctolite. These observations suggest that the Mg-rich component, regardless of the identity, is fine grained. There is no hint, however, of Mg enrichment in the fine grain size fractions of soil sample 76501 in the study of Laul et al. (1981). For the model discussed here, we use the 76535 troctolite to represent the Mg-rich component of the station 6 regolith with the caveat that some other cryptic but almost certainly mafic, nonmare lithology may be the actual culprit. Compositions of all tested model components are presented in Table S3.

Models that include the 76535 troctolite as the mafic, high-Mg' component require 8–17% troctolite by mass, increasing with decreasing Mg' of the assumed anorthositic norite component. In all five models, the sum of the anorthositic norite and troctolite components, hereafter the "total feldspathic component," is nearly

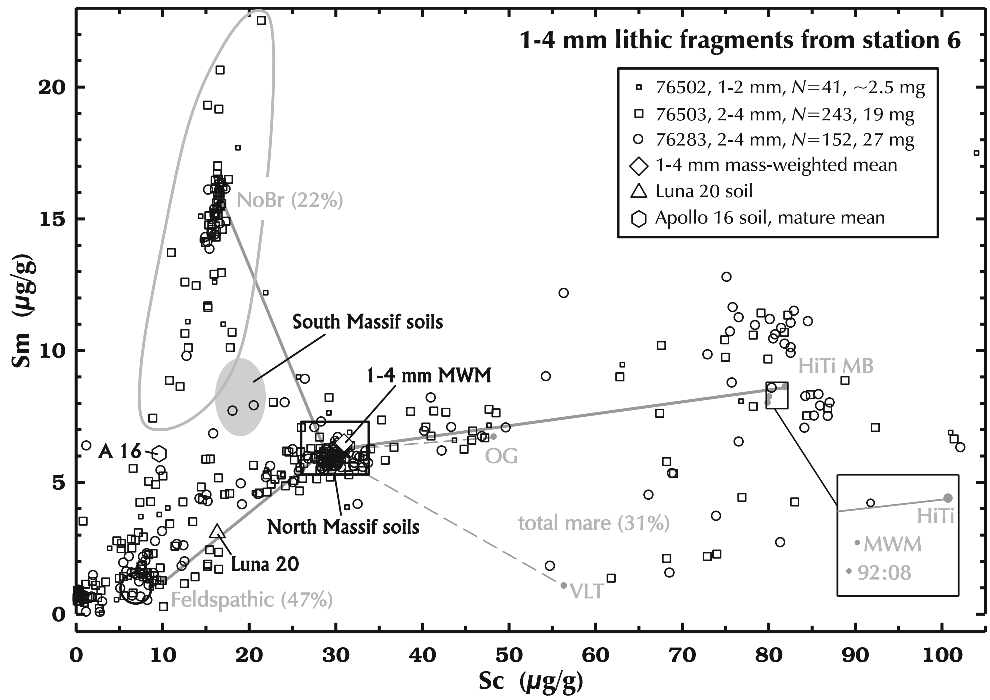

Fig. 3. Each square or circle point represents a 1–4 mm lithic fragment from station 6 samples 76502 (1–2 mm; Blanchard et al., 1975), 76503, and 76283 (2–4 mm; Jolliff et al., 1996). Mean masses of the fragments in each sample are presented in the legend. The rectangle at (30,6) represents the range of the station 6 soils of Fig. 5; the diagonal square in the rectangle represents the mass-weighted mean (MWM) composition of all 1–4 mm fragments, a composition that is very similar to that of the mean of the seven station 6 surface and trench soils (<1 mm; convergence of the diagonal lines). The large number of points in the rectangle represents regolith breccias. For reference, the diagonal lines are mixing lines between the mean composition of the seven station 6 surface and trench soils (Fig. 5) and (1) the KREEP-bearing, noritic breccia (NoBr) model component; (2) representing the maria, the high-Ti mare basalt (solid line), VLT basalt (dashed), and orange glass (OG, dashed) model components; and (3) the inferred mean composition of the total feldspathic component of the station 6 soils (Table 2). The percentage values associated with each mixing trend are those of the revised mixing model of Table 1 ("this work"). The inset at the lower right, in addition to the high-Ti basalt component, shows (1) the composition of the actual basalt component used in the modeling, a 92:08 mixture of high-Ti and VLT basalt; and (2) the MWM of the 62 most basaltic 1–4 mm lithic fragments. Soils from the South Massif, which contain less mare and feldspathic material than those of the North Massif, are represented by the gray ellipse (Korotev & Kremser, 1992). The hexagon represents the mean composition of mature soils of Apollo 16 (Korotev, 1997). They plot at low Sc because there is little mare material at Apollo 16. The large, obscured circle at (7,1) represents the composition of the typical crust of the feldspathic highlands as inferred from feldspathic lunar meteorites (Korotev & Irving, 2021). The triangle represents the composition of soil from Luna 20 (Fig. 6) (data of Lucey et al., 2006). HiTiMB = high-Ti mare basalt.

constant at 44–49%. Knowing the proportions, we can then calculate by difference the major element composition of the feldspathic components that yields ideal mass balance in each of the five models. For example, the five calculated Al_2O_3 concentrations are 24.5%, 26.0%, 24.4%, 25.1%, and 25.0% for the total feldspathic component, leading to a mean and uncertainty of 25.0 ± 0.4% (Table 2). The calculated composition is substantially more mafic and magnesian than either (1) typical regolith of the FHT (Feldspathic Highlands Terrane; Jolliff et al., 2000) as estimated from numerous feldspathic lunar meteorite (29.6% Al_2O_3 and Mg' = 65.5; Table 3) or (2) the feldspathic component of the Apollo 16 regolith (29.0% Al_2O_3 and Mg' = 69; Korotev, 1997, table 7). Because it is a mixture of all the low-Sc, low-Sm lithologies of the station 6 regolith, the composition of the total feldspathic component (Mg' = 78, 74 vol% plagioclase, olivine:pyroxene = 55:45; Table 2) has no petrologic significance but is that of an anorthositic troctolite, one plotting near the anorthositic norite join on the classification diagram of Stöffler et al. (1980).

The fraction of the total feldspathic component that is anorthositic norite ranges from 61% to 82% among the five models. The mean major element composition of the anorthositic norite component of the station 6 regolith (26.6% Al_2O_3 and Mg' = 70 ± 4, Table 3) is more mafic (~78 normative vol% plagioclase, Table 3) than either typical feldspathic lunar meteorites (85 vol %) or the feldspathic component of Apollo 16 soil

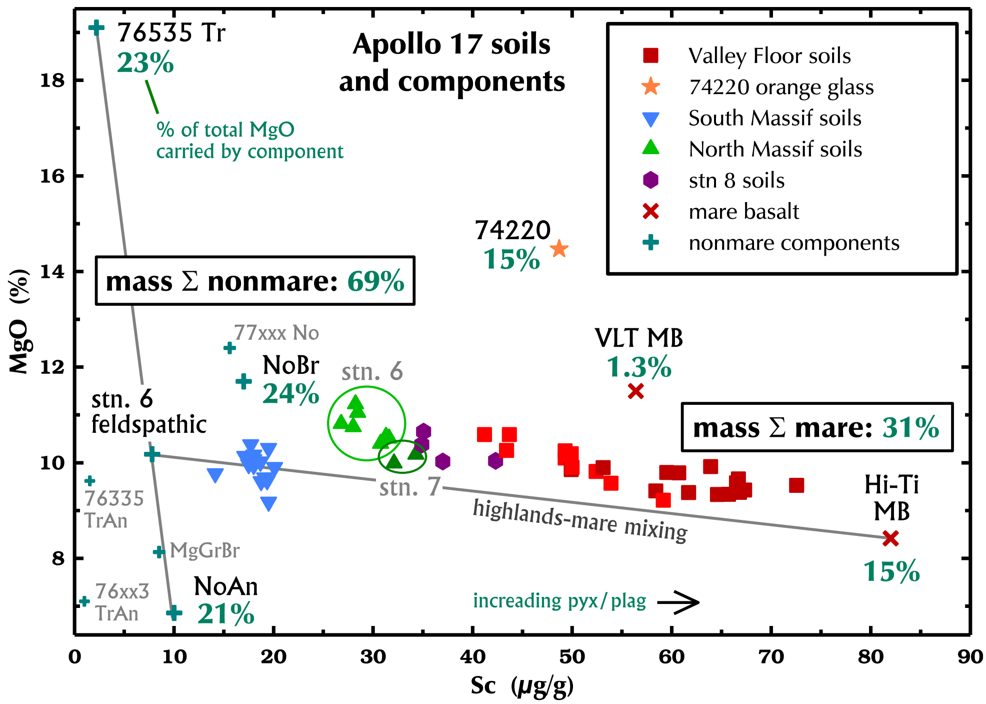

Fig. 4. Concentrations of MgO in Apollo 17 soils and lithologic (model) components of the soil. The highlands–mare mixing line is defined by the total feldspathic component of Table 2 (+ symbol at (8.0,10.2)) and the high-Ti mare basalt (MB) component (Table S3). Most soils of intermediate to high Sc concentration plot above the mixing line because they contain a significant proportion (10–20%) of picritic orange pyroclastic glass, represented here by soil sample 74220. Soils from station 6 are anomalously rich in MgO. Orange glass is an unlikely cause of the excess MgO as the station 6 soil contains only 31% mare material (Table 1) and soil from nearby (0.5 km) station 7 is not as anomalous. The excess cannot derive from KREEP-bearing, noritic impact melt breccias (NoBr) because such breccias are relatively more abundant at the South Massif than the North Massif (Fig. 3) and the South Massif soils (stations 2, 2A, and 3) do not have an excess of MgO. Feldspathic, magnesian lithologies such as troctolitic anorthosite (TrAn) 76335 (Mg' = 87), the troctolitic anorthosite occurring in soil samples 76503 and 76283 ("76xx3," Jolliff et al., 1992, 1996), and Apollo 17 magnesian granulitic breccia (MgGrBr, Mg' = 73) as well as norite (No) such as those collected at station 7 (samples 77075, 77077, and 77215) do not contain enough MgO to cause the MgO excess in the station 6 soil. Only a mafic, magnesian lithology such as troctolite 76535, which was collected as a rake sample from the station 6 regolith, is sufficiently rich in MgO to account for the MgO enrichment in the station 6 soils (mainly samples 76501, 76241, 76261, and 76281; Fig. 1). Compositionally, the inferred total feldspathic component of the station 6 soils (Table 2) is a 73:27 mixture of the noritic anorthosite (NoAn, Mg' = 70) and the 76535 troctolite (Tr, Mg' = 87). Values in percent are the fractions of the total MgO in the station 6 soil carried by each of the major model components. The 72415 dunite plots off scale at (4,39). (Color figure can be viewed at wileyonlinelibrary.com.)

(91%). The composition is approximately equivalent to a 40:60 mixture of Apollo 17 ferroan granulitic breccia and magnesian granulitic breccia and is much like that of some lunar meteorites of anorthositic noritic composition, for example, Pecora Escarpment 02007 and Dhofar 1673 (Hill et al., 2018; Joy et al., 2010; Korotev et al., 2006). Note that with 78 vol% plagioclase (Table 3), the "anorthositic norite" component is just on the line (77.5%) between the anorthositic norite and noritic anorthosite fields of Stöffler et al. (1980) and, in fact, is in the noritic anorthosite field.

Mass-balance models are imperfect in that the identity of the components is an input assumption, not a model prediction. The concentrations of TiO_2 in the high-Ti basalts and orange glass of Apollo 17 are well known (Neal & Taylor, 1992). In the model of Table 2, the basalt component (Table S3, itself a 92:08 mixture of high-Ti mare basalt and VLT basalt; Korotev & Kremser, 1992) contributes about 68% and the orange glass 28% of the TiO_2 in the station 6 regolith. Yet among the five anorthositic norite components tested, all models overestimate the concentration of TiO_2 in the soils by 5–15% of the observed TiO_2 concentration value. Similarly, all models overestimate the concentrations of light REE La and Ce by 3–4%. The implication is that there is an unidentified but volumetrically significant basaltic (?) lithology in the station 6 regolith that is lower in TiO_2 than the 92:08 basalt model component and perhaps slightly poorer in light REE relative to heavy REE. Mass balance for TiO_2 can be achieved, however,

Table 2. Estimated major element composition and normative mineralogy of the total feldspathic component of the station 6 regolith with comparison to the estimated composition of the nonmare component of the Luna 20 regolith.

	Luna 20	Station 6			
	%	%		Mass %	Vol%
SiO_2	45.2	44.47	Plag	69.5	73.8
TiO_2	~0	0.21	Pyr	13.2	11.5
Al_2O_3	24.8	25.0	Ol	16.6	14.0
Cr_2O_3	0.17	0.123	Ilm	0.40	0.25
FeO_T	4.8	5.34	Chr	0.18	0.10
MnO	0.09	0.077	Ksp	0.24	0.27
MgO	10.0	10.18	Ap	0.07	0.06
CaO	14.9	14.21			
Na_2O	0.34	0.288			
K_2O	0.06	0.04			
P_2O_5	—	0.03			
Σ	100.5	100.0		100.2	100.0
Mg′	79.	77.6			

Normative mineralogy from Excel® spreadsheet of Hollocher (2022). The Luna 20 composition is that inferred from Fig. 5, that is, the Luna 20 soil composition minus the component(s) of mare basalt. FeO_T = total Fe as FeO, Plag = plagioclase, Pyr = total pyroxenes, Ol = olivine, Ilm = ilmenite, Chr = chromite, Ksp = potassium feldspar, Ap = apatite.

Table 3. Estimated major element composition and normative mineralogy of the anorthositic norite component of the station 6 regolith with comparison to the estimated typical composition of the Feldspathic Highlands Terrane.

	FHT	Station 6				
	%	%	±		Mass%	Vol%
SiO_2	44.2	45.1	0.4	Plag	73.9	78.0
TiO_2	0.184	0.27	0.06	Pyr	17.1	14.6
Al_2O_3	29.55	26.6	1.4	Ol	8.1	6.6
Cr_2O_3	0.080	0.13	0.03	Ilm	0.51	0.31
FeO_T	3.90	5.3	0.8	Chr	0.19	0.11
MnO	0.061	0.081	0.009	Ksp	0.24	0.27
MgO	4.33	6.8	1.6	Ap	0.07	0.06
CaO	16.7	15.3	0.6			
Na_2O	0.343	0.312	0.016			
K_2O	0.028	0.044	0.007			
P_2O_5	0.029	0.030	0.006			
Σ	99.8	100.0			100.1	100.0
Mg′	65.5	70.	4.			

Uncertainties (±) = 95% confidence limits. Normative mineralogy from Excel® spreadsheet of Hollocher (2022). The FHT composition is the estimate of Korotev and Irving (2021) based on major element data for 24 typical feldspathic lunar meteorites.
FeO_T = total Fe as FeO.

with a mare basalt component that is an 81:19 mixture of high-Ti basalt and VLT basalt, but there is no petrographic evidence for such a high proportion of VLT basalt in the station 6 regolith and the composition data for 1–4 mm basaltic lithic fragments also do not support such a high proportion of VLT basalt (Fig. 3, inset).

76001 Core

There are no layers of distinct composition in 76001 (Fig. 2) as there are in other Apollo cores that were taken on "horizontal" surfaces through overlapping deposits of ejecta from small craters (Korotev, 1991; Korotev et al., 1984; Korotev & Morris, 1993; Laul & Papike, 1980; Morris et al., 1989). The compositional data are consistent with the conclusion of Nagle (1979) that the core material, at least the <1 mm portion, was accumulated by continuous downslope mass wasting.

There is little to no hint in the composition data of the six stratigraphic units recognized by Nagle (1979), although some individual samples in the top portion of the core where large lithic fragments were observed by Nagle (1979) are slightly richer in Sc or Sm as a result of nuggets of mare basalt or KREEP-bearing noritic impact melt breccia (Fig. 2c and 2d). Overall, the core is more feldspathic than any of the station 6 surface and trench soils except for sample 76501, which was collected near the core and 20 m away from the boulder track (Fig. 1). Compared to 46.6% feldspathic component for the mean of the seven surface and trench soils from station 6 (Table 1), the top of the core (mean of top five samples) has 48.4 ± 1.0% and the bottom of the core (mean of bottom five samples) has 50.1 ± 1.0% on the basis of Sc and Sm concentrations (Figs. 3 and 5), that is, there is a slight increase with depth, particularly below 20 cm (Papike & Wyszynski, 1980) in feldspathic components while the other components maintain the same relative abundances. There is no systematic change in concentrations of Ni with depth (Fig. 2g), an observation consistent with mass wasting but not with in situ gardening by micrometeorites.

DISCUSSION

Source of the Nonmare Materials of the North Massif

There has been much discussion and little consensus about the source of the KREEP-bearing, noritic impact melt breccias of Apollo 17. The Serenitatis, Imbrium, and Crisium basins have each been advocated (Dalrymple & Ryder, 1996; Haskin, 1998; Haskin et al., 1998; Schmitt et al., 2017; Spudis & Ryder, 1981; Wieczorek et al., 1998). Most of the arguments have been based on photogeology, surface observations by the astronauts,

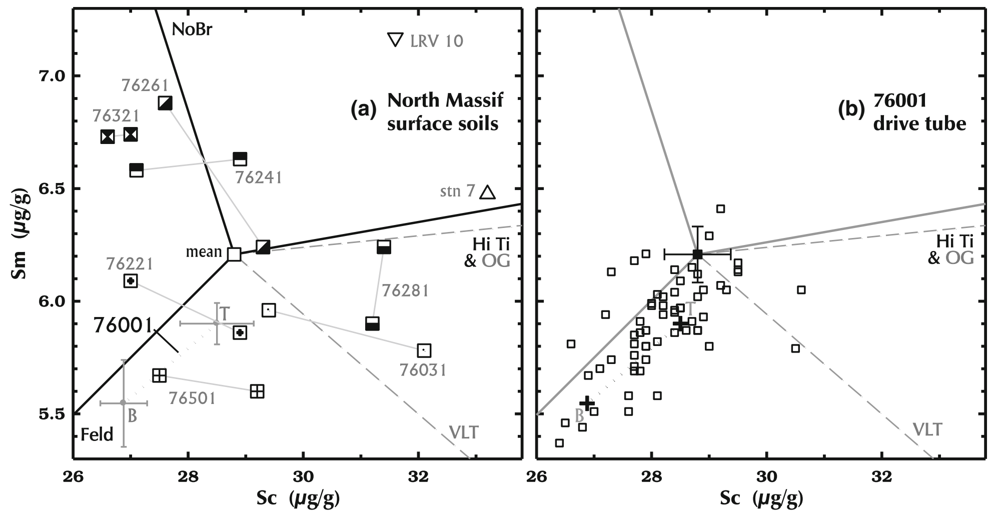

Fig. 5. Comparison of 76001 drive tube samples to the seven surface and trench soils of station 6 (Fig. 1) in Sc-Sm space. a) Two samples each (~50 mg) of the seven station 6 soils and comparison to soils from the other two North Massif sampling sites, LRV stop 10 (Turning Point Rock, about 0.5 km southwest and downslope from station 6) and station 7 (0.5 km east of station 6). The diagonal mixing lines are those of Fig. 3, where the convergence (unfilled square) is the mean of seven surface and trench soils. b) The dotted line is a linear regression to the 76001 data excluding the two high-Sc points (Fig. 2). The "T" represents the mean of the top five samples (0–3 cm) and the "B" represents the mean of the bottom five samples (29–32 cm) of the core, with 95% confidence limits. Surface samples 76221 (in boulder track) and 76501 (30 m west of boulders) are most similar to the 76001 core; samples collected near the boulders tend to be richer in the noritic breccia. Overall, the core soil is more feldspathic than the mean of the station 6 surface soils and becomes more feldspathic with depth.

composition, petrography, and geochronology of returned rock samples, and composition and mineralogy of the lunar surface as determined from orbit. The most recent synthesis of the available information is that of Hurwitz and Kring (2016). Here, we present some largely overlooked observations and constraints based mainly on regolith composition.

Rhodes et al. (1974) advocated a model in which the Apollo 17 massifs were stratigraphically similar to each other with KREEP-rich, noritic impact melt overlying KREEP-poor feldspathic material. The soils of stations 2 and 3 at the base of the South Massif are richer in the melt breccia component (45–50% of the nonmare material, Fig. 3) because they were sampled on the light mantle avalanche deposit that originated from the top of the massif. The avalanche is relatively recent (15–50 My; Wolfe et al., 1975); thus, there has been little contamination of the deposit with mare material (6–9% at stations 2 and 3; Korotev & Kremser, 1992; Rhodes et al., 1974) since its emplacement. At the North Massif, a smaller fraction of the nonmare portion of the regolith contains noritic impact melt, ~32% (=22.1/(22.1 + 46.6), Table 1), because the regolith is dominated by KREEP-poor feldspathic material from the lower portion of the massif.

Regolith composition does not support some suggestions regarding Crisium and Imbrium ejecta at Apollo 17. Based in part on the observations and conclusions of Haskin (1998) and Haskin et al. (1998), Spudis et al. (2011) recognized that the KREEP-bearing melt breccias of the Apollo 17 massifs may not be from nearby Serenitatis but from more distant but younger Imbrium. Specifically, they advocated that the Sculptured Hills as sampled at station 8 (2.25 km east of station 6) is an Imbrium basin deposit. None of the six nonmare rocks sampled at station 8, however, are KREEP-rich impact melt breccias such as those found at the North and South Massifs or those associated with Imbrium at Apollo 12, 14, 15, and 16 (Korotev, 2000). One is a 400 g ferroan granulitic breccia of anorthositic norite composition, sample 78155 (13 $\mu g\ g^{-1}$ Sc and 1.8 $\mu g\ g^{-1}$ Sm). Another, sample 78527, is a 5 g breccia from the regolith with a magnesian norite composition (8–9 $\mu g\ g^{-1}$ Sc and ~ 4 $\mu g\ g^{-1}$ Sm). The remaining four (samples 78235, 78236, 78238, and 78255) are shocked but unbrecciated magnesian-suite norites (12 $\mu g\ g^{-1}$ Sc, 1.2–2 $\mu g\ g^{-1}$ Sm), all fragments from a 0.5 m boulder lying on the surface (composition data from Meyer, n.d.: The Lunar Sample Compendium). The boulder may not be typical of the mafic, nonmare lithologies of the Sculptured Hills, however (Petro et al., 2015). Among the 39 lithic fragments (1–2 mm) from the regolith of station 8 in the study of Blanchard et al. (1975), 14 are largely nonmare in having <25 $\mu g\ g^{-1}$ Sc, but none has the composition of a KREEP-rich impact melt breccia (e.g., [Sm,FeO] = [16 ± 2,9 ± 1]) and only two are consistent with the 78235 norite composition (fig. 2 of Blanchard et al., 1975). At station 8, 56% of the <1 mm regolith (compared to 69% at station 6; Table 1) is nonmare material, but only 28% of that material is KREEP-bearing noritic impact melt breccia by mass balance, essentially the same as at station 6 (32%). In summary, there is no compositional evidence among regolith samples that the nonmare component of the Sculptured Hills is substantially different from that of the North Massif. The noritic impact melt breccias may be Imbrium ejecta, but there is no compositional evidence that the breccias differ between station 6 and station 8.

More recently, Schmitt et al. (2017) suggested that the KREEP-bearing, station 6 boulder is possibly of Crisium origin while the station 7 boulder is from Serenitatis. Despite the slight age difference (table 1 of Schmitt et al., 2017), the Crisium hypothesis is unlikely because (1) there is no evidence in the Th data from Lunar Prospector for the existence of KREEP in the Crisium target area (Lawrence et al., 2003), (2) the Luna 20 regolith is not rich in incompatible elements (below), and (3) the station 7 boulders are compositionally indistinguishable from the station 6 boulders (Norman et al., 2002). The composition of the station 7 soil corresponds well to a 90:10 mixture of station 6 regolith and mare basalt.

Less emphasis has been put on the source of the KREEP-poor feldspathic material at Apollo 17. Impact models predict the occurrence of ejecta from Imbrium, Nectaris, Crisium, as well as Serenitatis at the Apollo 17 site (McGetchin et al., 1973; Petro & Pieters, 2008) and we might expect ejecta from each of these basins to include some feldspathic material. The composition of anorthositic norite component of the North Massif (Table 3), however, is not typical of the FHT. As noted above, it is more mafic (74 mass% normative plagioclase) than typical feldspathic lunar meteorites (82%; Korotev & Irving, 2021) or the feldspathic material of the Apollo 16 regolith (89%). The main peculiarity of the feldspathic (nonmare, non-KREEP) material of the North Massif, however, is the apparent presence of a troctolite component that leads to a highly magnesian, anorthositic troctolite composition (Mg' = 78, Table 2) compared to typical feldspathic highlands (65.5 ± 2.1; Korotev & Irving, 2021). Some lunar meteorites are anorthositic troctolite in composition, with Mg' as high as 78 in the Northwest Africa 5744 clan (~20 vol% olivine and 11 vol% pyroxene; Korotev & Irving, 2021) but none are as mafic as troctolite 76535 (35–37 vol% Fo_{87} olivine, and 4–5 vol% orthopyroxene; Dymek et al., 1975; Gooley et al., 1974; Warren, 1993).

Luna 20 Connection

Three robotic Soviet Luna missions collected regolith samples with drill cores near the equator (0.7°S to 12.7°N) on the eastern (56–62°E) nearside of the Moon in 1970, 1972, and 1976. Luna 16 sampled Mare Fecunditatis and Luna 24 sampled Mare Crisium. Luna 20 landed in the Apollonius highlands between the two mare sites but closer to Mare Fecunditatis. The Luna 20 regolith is believed to be largely ejecta from the younger Crisium basin (Swindle et al., 1991; Wilhelms, 1987).

The petrography and mean composition of the feldspathic lithologies of the Apollo 17 North Massif resemble those of Luna 20 more than they do those of Apollo 16 or typical feldspathic highlands (Figs. 3 and 6). At Luna 20, nonmare rocks are not as rich in incompatible elements as at Apollo 16 (Fig. 6) (Taylor et al., 1973). Fragments of highly feldspathic (>90% plagioclase) anorthosite are not common at Luna 20 (Fig. 6) (Taylor et al., 1973), but Mg-rich rocks like anorthositic troctolite, troctolite, and spinel troctolites are common (Brett et al., 1973; Cameron et al., 1973; Meyer, 1973; Prinz et al., 1973; Reid et al., 1973; Roedder & Weiblen, 1973; Simon et al., 1981). Like the North Massif regolith, feldspathic granulitic breccias are common in the Luna 20 regolith ("recrystallized anorthositic norite and anorthositic troctolite," Cameron et al., 1973; "One third of the fragments of microbreccia have undergone thermal metamorphism," Kridelbaugh & Weill, 1973; "The textures now observed in these fragments are in large part metamorphic," Roedder & Weiblen, 1973).

Like the regolith of the North Massif, the Luna 20 regolith contains some mare basalt. Basalt flows are exposed 250 km to the north of the Luna 20 landing site in Mare Crisium and 50 km to the south in Mare Fecunditatis. Basaltic lithic fragments, mineral grains, and glass are observed in the Luna 20 regolith (Cameron et al., 1973; Glass, 1973; Kridelbaugh & Weill, 1973; Michel-Lévy & Johan, 1973; Roedder & Weiblen, 1973). We observe at least three basalt-bearing breccias among the 14 small Luna 20 agglutinate and regolith breccias that we have studied (0.12–1.00 mg, Table 2; Fig. 6).

The proportion of mare material in the Luna 20 regolith can easily be estimated as 16–17%. The Sc concentration of Luna 20 soil is 16 $\mu g\ g^{-1}$ and Mg' is 70 (Lucey et al., 2006). From the geometries of Figs. 3 and 6, we can reasonably assume that the nonmare component of the Luna 20 regolith contains <16 $\mu g\ g^{-1}$ Sc. If we also assume that the basalt component is like the aluminous basalts of Luna 16 (Mare Fecunditatis), then by mass balance, Sc in the nonmare component is 7 $\mu g\ g^{-1}$, Mg' is 77.5, the regolith contains 16% mare basalt, and the

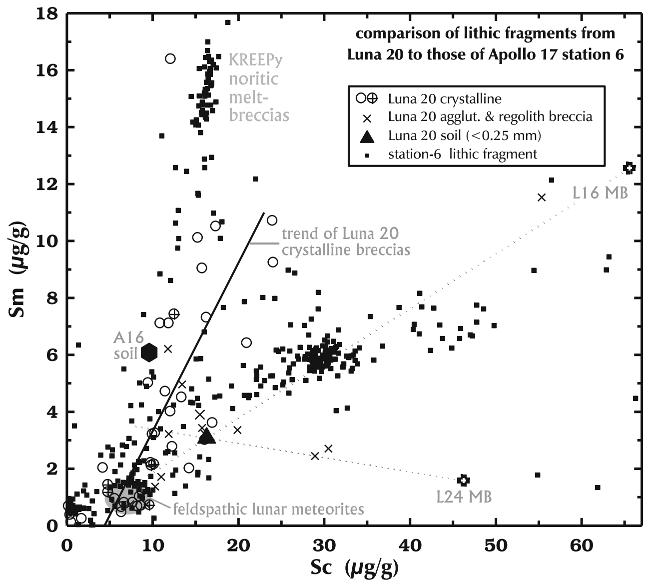

Fig. 6. Comparison of lithic fragments from station 6 of Apollo 17 (small squares, from low-Sc portion of Fig. 3) to those from Luna 20 ($N = 56$; mass range: 0.12–6.0 mg; data of Laul & Schmitt [1973], $N = 3$; Jérome & Philipott [1973], $N = 6$; Smith et al. [1983], $N = 25$; Swindle et al. [1991], $N = 6$; and this work, $N = 25$) (Table S2). The six circles with + symbols in the center are the impact melt breccias of Swindle et al. (1991) for which ^{40}Ar-^{39}Ar ages were determined. Five of these are feldspathic with 5–10 µg g^{-1} Sc and 0.7–2.2 µg g^{-1} Sm (largely obscured). None of the six melt breccias of Swindle et al. (1991) have Sc and Sm concentrations as high as the KREEP-bearing, noritic impact melt breccias of Apollo 17 but one of the crystalline breccias not identified as a melt breccia microscopically is similar. Only three of the Luna 20 fragments have low Sc (<2 µg g^{-1}) and Sm (<1 µg g^{-1}) such as observed in Apollo 16 ferroan anorthosite. At least three of the "agglutinates and regolith breccias" of Luna 20 are rich in Sc from mare material; one (55 µg g^{-1} Sc) is similar to the Luna 16 mare basalt and the other two (~30 µg g^{-1} Sc) appear to have a component of Lunar 24 VLT basalt. The solid diagonal line is a fit to the crystalline breccias of Luna 20, excluding the one high-Sm point. The dotted lines are defined by (1) the mean composition of the Luna 20 soil (large triangle, Table S3) and (2) the aluminous basalt of Luna 16 or the VLT mare basalt of Luna 24 (Table S3). Extrapolating these lines to the crystalline-breccia line implies that the nonmare component of Luna 20 soils has 7 µg g^{-1} Sc (assuming Luna 16 basalt) or 10 µg g^{-1} (assuming Luna 24 basalt). The mean of the compositions represented by these two intersection points is the Luna 20 nonmare composition of Table 2.

nonmare portion has 72 vol% normative plagioclase (Fig. 6). Alternately, if we assume the basalt component is like the VLT basalts of Luna 24 (Mare Crisium), then Sc in the nonmare component is 10 µg g^{-1}, Mg' is 80, the regolith contains 17% mare material, and the nonmare component is 73 vol% normative plagioclase (Fig. 6). Both of these high Mg' values, as well as the concentrations of all major elements, are similar to that of the total feldspathic component of the North Massif ($Mg' = 77.6$, Table 2) and both compositions (12–13 vol % olivine compared with 13.9% at the North Massif, Table 2) correspond to anorthositic troctolite (Stöffler et al., 1980).

These various similarities between the nonmare lithologies of the Apollo 17 North Massif and Luna 20 site suggest that both sites are dominated by basin ejecta that is considerably more mafic and magnesian than typical of the surface of the feldspathic highlands as inferred from numerous feldspathic lunar meteorites and that either (1) the prebasin, lower feldspathic crust in the vicinity of the Serenitatis and Crisium basins were similar to each other or (2) the same KREEP-poor basin ejecta occurs at both sites. The two sites are 910 km apart, 8% of the lunar circumference.

SUMMARY AND CONCLUSIONS

On the basis of compositional mass balance about half of the material in the regolith of station 6 at the base of the Apollo 17 North Massif is feldspathic and poor in incompatible elements. Such material dominates the lower slope of the massif. The other half consists of material derived from the local mare (~30%) and KREEP-bearing, noritic impact melt breccia (~20%) mainly from the top of the massif. On average, the composition of regolith of the 31 cm long 76001 drive tube is similar to that of the seven samples of surface and trench soil taken at station 6 but is at the compositionally feldspathic end of the range. The core regolith is uniform in composition with depth, but there is a slight increase in the proportion of feldspathic material from the top of the core (48%) to the bottom (50%). No layers of distinct composition occur as, for example, are observed in the deep drill core or the drive tube from station 9, both taken on the Taurus–Littrow valley floor (Laul et al., 1979; Morris et al., 1989). The composition data are consistent with conclusions of previous studies that the core material derived from downslope mass wasting of fine material from higher on the massif, not as ejecta of nearby craters.

Previous petrographic studies have shown the feldspathic material of the North Massif to include a variety of lithologies including ferroan (low Mg') and magnesian (high Mg') granulitic breccias, ferroan anorthosite, magnesian troctolitic anorthosite, and feldspathic impact melt breccias. These lithologies alone, however, cannot account for the high mean MgO concentration of the nominally feldspathic component of the station 6 regolith. The feldspathic component must also consist of about 27% of a Mg-rich lithology such as troctolite sample 76535. Although the troctolite was collected as a rock (155.5 g) from the station 6 regolith, no rocks as mafic as 76535 have been observed in petrographic studies of the station 6 regolith. The bulk composition of the feldspathic material in the station 6 regolith is that of an anorthositic troctolite (74 vol% plagioclase, 14 vol% olivine, and 12 vol%. pyroxene) with high *Mg′*, 77.6. The mineralogy and composition are considerably more mafic and magnesian than the feldspathic component of the Apollo 16 regolith, the regolith of the South Massif as exposed on the light mantle, or typical regolith of the Feldspathic Highlands Terrane as inferred from numerous feldspathic lunar meteorites. It is, however, nearly identical to that of the nonmare portion of the Luna 20 regolith on the ejecta deposit of the Crisium basin.

Regolith and rock compositions do not support hypotheses that the Sculptured Hills at station 8 or the boulder of station 7 are composed of lithologies significantly different in origin than those of station 6.

Acknowledgments—This work was supported by NASA through grants NAG 9-56 and NAGW-3343 and the McDonnell Center for the Space Sciences, Washington University in St. Louis. The author greatly appreciates the constructive reviews of Noah Petro, Natalie Curran, and associate editor Katherine Joy.

Data Availability Statement—Data available in article supplementary material.

Editorial Handling—Dr. Katherine Helen Joy

REFERENCES

Allton J. H. 1989. *Catalog of Apollo Lunar Surface Geological Sampling Tools and Containers*, JSC-23454. Houston, Texas: NASA Johnson Space Center.

Bell, S. K., Joy, K. H., Nottingham, M., Tartèse, R., Jones, R. H., Kent, J. J., Shearer, C. K., and the ANGSA Science Team. 2022. Initial Petrographic Analysis of Apollo 17 73002 Continuous Core Thin Sections Using QEMSCAN Mapping Techniques (Abstract #1947). 53rd Lunar and Planetary Science Conference. CD-ROM.

Blanchard, D. P., Korotev, R. L., Brannon, J. C., Jacobs, J. W., Haskin, L. A., Reid, A. M., Donaldson, C. H., and Brown, R. W. 1975. A Geochemical and Petrographic Study of 1–2 mm Fines from Apollo 17. Proceedings, 6th Lunar Science Conference. pp. 2321–41.

Brett, R., Gooley, R. C., Dowty, E., Prinz, M., and Keil, K. 1973. Oxide Minerals in Lithic Fragments from Luna 20 Fines. *Geochimica et Cosmochimica Acta* 37: 761–73.

Cameron, K. L., Papike, J. J., Bence, A. E., and Sueno, S. 1973. Petrology of Fine-Grained Rock Fragments and Petrologic Implications of Single Crystals from the Luna 20 Soil. *Geochimica et Cosmochimica Acta* 37: 775–93.

Dalrymple, G. B., and Ryder, G. 1996. Argon-40/Argon-39 Age Spectra of Apollo 17 Highlands Breccia Samples by Laser Step Heating and the Age of the Serenitatis Basin. *Journal of Geophysical Research* 101: 26069–84.

Dymek, R. F., Albee, A. L., and Chodos, A. A. 1975. Comparative Petrology of Lunar Cumulate Rocks of Possible Primary Origin: Dunite 72415, Troctolite 76535, Norite 78235, and Anorthosite 62237. Proceedings, 6th Lunar Science Conference. pp. 301–41.

Elsila, J. E., Aponte, J. C., Dworkin, J. P., Glavin, D. P., McLain, H. L., Simkus, D. N., and the ANGSA Science Team. 2022. Trace Levels of Volatile Organic Compounds and Cyanide in the Apollo 73002 Core Sample (Abstract #1212). 53rd Lunar and Planetary Science Conference. CD-ROM.

Fruchter, J. S., Evans, J. C., Reeves, J. H., and Perkins, R. W. 1980. Depositional History of the Apollo Drive Tube 76001 During the Past Few Million Years (Abstract). 11th Lunar and Planetary Science Conference. pp. 306–8.

Glass, B. P. 1973. Major Element Compositions of Luna 20 Glass Particles. *Geochimica et Cosmochimica Acta* 37: 841–6.

Gooley, R. C., Brett, R., Warner, J. L., and Smyth, J. R. 1974. A Lunar Rock of Deep Crustal Origin: Sample 76535. *Geochimica et Cosmochimica Acta* 38: 1329–39.

Haskin, L. A. 1998. The Imbrium Impact Event and Thorium Distribution at the Lunar Highlands Surface. *Journal of Geophysical Research* 103: 1679–89.

Haskin, L. A., Korotev, R. L., Rockow, K. M., and Jolliff, B. L. 1998. The Case for an Imbrium Origin of the Apollo Th-Rich Impact-Melt Breccias. *Meteoritics & Planetary Science* 33: 959–75. https://doi.org/10.1111/j.1945-5100.1998.tb01703.x.

Haskin, L. A., Shih. C.-Y., Bansal. B. M., Rhodes. J. M., Wiesmann. H., and Nyquist. L. E. 1974. The Evidence for the Origin of 76535 as a Cumulate. Proceedings, 5th Lunar Science Conference. pp. 1213–25.

Hill, P. J. A., Osinski, G. R., Banerjee, N. R., Korotev, R. L., Nasir, S. J., and Herd, C. D. K. 2018. Petrography and Geochemistry of Lunar Meteorites Dhofar 1673, 1983, and 1984. *Meteoritics & Planetary Science* 54: 300–20. https://doi.org/10.1111/maps.13207.

Hollocher, K. T. 2022. Norm Calculation Program. Accessed January 4, 2022. https://zenodo.org/record/5818037#.Yf6s8erMLJ4.

Hurwitz, D., and Kring, D. A. 2016. Identifying the Context of the Apollo 17 Impact Melt Breccia. *Earth and Planetary Science Letters* 436: 64–70. https://doi.org/10.1016/j.epsl.2015.12.032.

Jérome, D. Y., and Philipott, J.-C. 1973. Chemical Composition of Luna 20 Soil and Rock Fragments. *Geochimica Cosmochimica Acta* 37: 909–14.

Jolliff, B. L., Bishop, K. M., and Haskin, L. A. 1992. Possible Petrogenetic Associations Among Igneous Components in North Massif Soils: Evidence in 2-4-mm Soil Particles from 76503. In *Workshop on Geology of the Apollo 17 Landing Site, Part 1*, edited by G. Ryder, H. H. Schmitt, and P. D. Spudis, 24–26. LPI Technical Report 92-09. Houston, Texas: Lunar and Planetary Institute.

Jolliff, B. L., Gillis, J. J., Haskin, L. A., Korotev, R. L., and Wieczorek, M. A. 2000. Major Lunar Crustal Terranes: Surface Expressions and Crust-Mantle Origins. *Journal of Geophysical Research* 105: 4197–216.

Jolliff, B. L., Rockow, K. M., Korotev, R. L., and Haskin, L. A. 1996. Lithologic Distribution and Geologic History of the Apollo 17 Site: The Record in Soils and Small Rock

Particles from the Highlands Massifs. *Meteoritics & Planetary Science* 31: 116–45.

Joy, K. H., Crawford, I. A., Russell, S. S., and Kearsley, A. T. 2010. Lunar Meteorite Regolith Breccias: An In Situ Study of Impact Melt Composition Using LA-ICP-MS with Implications for the Composition of the Lunar Crust. *Meteoritics & Planetary Science* 45: 917–46. https://doi.org/10.1111/j.1945-5100.2010.01067.x.

Korotev, R. L. 1991. Geochemical Stratigraphy of Two Regolith Cores from the Central Highlands of the Moon (Abstract). 21st Lunar and Planetary Science Conference. pp. 229–89.

Korotev, R. L. 1997. Some Things We Can Infer About the Moon from the Composition of the Apollo 16 Regolith. *Meteoritics & Planetary Science* 32: 447–78.

Korotev, R. L. 2000. The Great Lunar Hot Spot and the Composition and Origin of the Apollo Mafic ("LKFM") Impact-Melt Breccias. *Journal of Geophysical Research* 105: 4317–45. https://doi.org/10.1029/1999JE001063.

Korotev, R. L., and Bishop, K. M. 1993. Composition of Apollo 17 Core 76001 (Abstract). 24th Lunar and Planetary Science Conference. p. 1411.

Korotev, R. L., and Haskin, L. A. 1988. Compositional Survey of Particles from the Luna 20 Regolith (Abstract). 19th Lunar and Planetary Science Conference. pp. 635–6.

Korotev, R. L., and Irving, A. J. 2021. Lunar Meteorites from Northern Africa. *Meteoritics & Planetary Science* 56: 206–40. https://doi.org/10.1111/maps.13617.

Korotev, R. L., Jolliff, B. L., and Haskin, L. A. 1988. Compositional Survey of Particles from the Luna 16 Regolith (Abstract #1320). 19th Lunar and Planetary Science Conference. pp. 637–8.

Korotev, R. L., Jolliff, B. L., and Haskin, L. A. 1990a. Compositional Survey of Particles from the Luna 16 Regolith, Part 2 (Abstract #1338). 19th Lunar and Planetary Science Conference. pp. 662–3.

Korotev, R. L., Jolliff, B. L., and Haskin, L. A. 1990b. Compositional Survey of Particles from the Luna 24 Regolith (Abstract #1339). 19th Lunar and Planetary Science Conference. pp. 664–5.

Korotev, R. L., and Kremser, D. T. 1992. Compositional Variations in Apollo 17 Soils and Their Relationship to the Geology of the Taurus-Littrow Site (Abstract). 22nd Lunar and Planetary Science Conference. pp. 275–301.

Korotev, R. L., and Morris, R. V. 1993. Composition and Maturity of Apollo 16 Regolith Core 60013/14. *Geochimica et Cosmochimica Acta* 57: 4813–26.

Korotev, R. L., Morris, R. V., and Lauer, H. V. Jr. 1984. Stratigraphy and Geochemistry of the Stone Mountain Core (64001/2) (Abstract). 15th Lunar and Planetary Science Conference. pp. C143–C160.

Korotev, R. L., Zeigler, R. A., and Jolliff, B. L. 2006. Feldspathic Lunar Meteorites Pecora Escarpment 02007 and Dhofar 489: Contamination of the Surface of the Lunar Highlands by Post-Basin Impacts. *Geochimica et Cosmochimica Acta* 70: 5935–56. https://doi.org/10.1016/j.gca.2006.09.016.

Kridelbaugh, S. J., and Weill, D. F. 1973. The Mineralogy and Petrology of the Luna 20 Soil Sample. *Geochimica et Cosmochimica Acta* 37: 915–26.

Laul, J. C., Lepel, E. A., Vaniman, D. T., and Papike, J. J. 1979. The Apollo 17 Drill Core: Chemical Systematics of Grain-Size Fractions (Abstract). 10th Lunar and Planetary Science Conference. pp. 1269–98.

Laul, J. C., and Papike, J. J. 1980. The Apollo 17 Drill Core: Chemistry of Size Fractions and the Nature of the Fused Soil Component (Abstract). 11th Lunar and Planetary Science Conference. pp. 1395–413.

Laul, J. C., Papike, J. J., and Simon, S. B. 1981. The Lunar Regolith: Comparative Studies of the Apollo and Luna Sites. Chemistry of Soils from Apollo 17, Luna 16, 20, and 24 (Abstract). 12th Lunar and Planetary Science Conference, Part B. pp. 389–407.

Laul, J. C., and Schmitt, R. A. 1973. Chemical Composition of Luna 20 Rocks and Soil and Apollo 16 Soils. *Geochimica Cosmochimica Acta* 37: 927–42.

Laul, J. C., and Schmitt, R. A. 1975. Dunite 72417: A Chemical Study. Proceedings, 6th Lunar Science Conference. pp. 1231–54.

Lawrence, D. J., Elphic, R. C., Feldman, W. C., Prettyman, T. H., Gasnault, O., and Maurice, S. 2003. Small-Area Thorium Features on the Lunar Surface. *Journal of Geophysical Research* 108: 5102. https://doi.org/10.1029/2003JE0020500.

Lucey, P., Korotev, R. L., Gillis, J. J., Taylor, L. A., Lawrence, D., Elphic, R., Feldman, B., Hood, L. L., Hunten, D., Mendillo, M., Noble, S., Papike, J. J., and Reedy, R. C. 2006. Understanding the Lunar Surface and Space-Moon Interactions. In *New Views of the Moon, Reviews in Mineralogy and Geochemistry*, edited by B. L. Jolliff, M. A. Wieczorek, C. K. Shearer, and C. R. Neal, vol. 60, 83–219. Washington, D.C.: Mineralogical Society of America.

McFadden, J. M., Thompson, M. S., Keller, L. P., Christoffersen, R., Morris, R. V., Shearer, C., and the ANGSA Science Team. 2022. Evaluating Space Weathering and Surface Exposure Timescales for Grains from Apollo 17 Core Sample 73001/73002 (Abstract #1539). 53rd Lunar and Planetary Science Conference. CD-ROM.

McGetchin, T. R., Settle, M., and Head, J. W. 1973. Radial Thickness Variation in Impact Crater Ejecta: Implications for Lunar Basin Deposits. *Earth and Planetary Science Letters* 20: 226–36.

Meyer, C. n.d. Lunar Sample Compendium. Accessed July 1, 2022. https://curator.jsc.nasa.gov/lunar/lsc/index.cfm.

Meyer, C., Jr., Brett, R., Hubbard, N. J., Morrison, D. A., McKay, D. S., Aitken, F. K., Takeda, H., and Schonfeld, E. 1971. Mineralogy, Chemistry, and Origin of the KREEP Component in Soil Samples from the Ocean of Storms. Proceedings, 2nd Lunar Science Conference. pp. 393–411.

Meyer, H. O. A. 1973. Luna 20: Mineralogy and Petrology of Fragments Less than 125 μm in Size. *Geochimica et Cosmochimica Acta* 37: 943–52.

Michel-Lévy, M. C., and Johan, Z. 1973. An Unusual Basalt Fragment in Luna 20 Sample L2010. *Geochimica et Cosmochimica Acta* 37: 805–9.

Morris, R. V., Gose, W. A., and Lauer, H. V. Jr. 1978. Depositional and Surface Exposure History of the Shorty Crater Core 74001/2: FMR and Magnetic Studies (Abstract). 9th Lunar and Planetary Science Conference. pp. 2033–48.

Morris, R. V., Korotev R. L., and Lauer H. V. Jr. 1989. Maturity and Geochemistry of the Van Serg Crater Core (79001/2) with Implications for Micrometeorite Composition (Abstract). 19th Lunar and Planetary Science Conference. pp. 269–84.

Morris, R. V., and Lauer, H. V. Jr. 1979. FeO and Surface Exposure (Maturity) Depth Profiles of Cores 15010/11 (Hadley Rille) and 76001 (North Massif) (Abstract). 10th Lunar and Planetary Science Conference. pp. 861–3.
Morris, R. V., Lauer, H. V. Jr., and Gose, W. A. 1979. Characterization and Depositional and Evolutionary History of the Apollo 17 Deep Drill Core (Abstract). 10th Lunar and Planetary Science Conference. pp. 1141–57.
Muehlberger, W. R., Batson, R. M., Cernan, E. A., Freeman, V. L., Halt, M. H., Halt, H. E., Howard, K. A. et al. 1973. Preliminary Geologic Investigation of the Apollo 17 Landing Site. In *Apollo 17 Preliminary Science Report*, pp. 6-1–6–91. NASA SP-330. Washington, DC: NASA.
Nagle, J. S. 1979. Drive Tube 76001—Continuous Accumulation with Complications? (Abstract). 10th Lunar and Planetary Science Conference. pp. 1385–99.
Nagle, J. S. 1982. An Ancient Avalanche Deposit in the Taurus-Littrow Valley Is Part of the Long Depositional History of the Apollo 17 Drill Core (Abstract). 12th Lunar and Planetary Science Conference, Part B. pp. 519–28.
Neal, C. R., and Taylor, L. A. 1992. Petrogenesis of mare basalts: A record of lunar volcanism. *Geochimica et Cosmochimica Acta* 56: 2177–211.
Neuman, M., Koefoed, P., Wang, K., Jolliff, B. L., Morris, R.V., and the ANGSA Science Team. 2022. Major and Trace Elemental Variations and Lithologic Component Analysis in Apollo 17 Drive Tube 73002 (Abstract #1567). 53rd Lunar and Planetary Science Conference. CD-ROM.
Norman, M. D., Bennett, V. C., and Ryder, G. 2002. Targeting the Impactors: Siderophile Element Signatures of Lunar Impact Melts from Serenitatis. *Earth and Planetary Science Letters* 202: 217–28.
Papike, J. J., and Wyszynski, J. 1980. Apollo 17 Drive Tube 76001: Modal Petrology (Abstract). 11th Lunar and Planetary Science Conference. pp. 1609–21.
Petro, N. E., Klima, R. L., and Ostrach, L. R. 2015. Constraining the Origin of Apollo 17's Station 8 Boulder: Implications for the Origin of the Sculptured Hills and the mg-Suite (Abstract #2687). 46th Lunar and Planetary Science Conference. CD-ROM.
Petro, N. E., and Pieters, C. M. 2008. The Lunar-Wide Effects of Basin Ejecta Distribution on the Early Megaregolith. *Meteoritics & Planetary Science* 43: 1517–29.
Prinz, M., Dowty, E., Keil, K., and Bunch, T. E. 1973. Mineralogy, Petrology, and Chemistry of Lithic Fragments from Luna 20 Fines: Origin of the Cumulate ANT Suite and Its Relationship to the High-Alumina and Mare Basalts. *Geochimica Cosmochimica Acta* 37: 979–1006.
Reid, A. M., Warner, J. L., Ridley, W. I., and Brown, R. W. 1973. Luna 20 Soil: Abundance and Composition of Phases in the 45–125 Micron Size Fraction. *Geochimica et Cosmochimica Acta* 37: 1011–30.
Rhodes, J. M., Rodgers, K. V., Shih, C., Bansal, B. M., Nyquist, L. E., Wiesmann, H., and Hubbard, N. J. 1974. The Relationships Between Geology and Soil Chemistry at the Apollo 17 Landing Site. Proceedings, 5th Lunar Science Conference. pp. 1097–117.
Roedder, E., and Weiblen, P. W. 1973. Petrology of Some Lithic Fragments from Luna 20. *Geochimica et Cosmochimica Acta* 37: 1031–52.
Schmitt, H. H. 2021. America's Uncommon Sense, the Website of Apollo 17 Astronaut, Senator Harrison H. Schmitt. Accessed January 15, 2021. https://www.americasuncommonsense.com/.
Schmitt, H. H., Petro, N. E., Wells, R. A., Robinson, M. S., Weiss, B. P., and Mercer, C. M. 2017. Revisiting the Field Geology of Taurus–Littrow. *Icarus* 298: 2–33.
Schwarz, C. 1987. Preliminary Description of Double Drive Tube 79002/79001 (Abstract). 18th Lunar and Planetary Science Conference. pp. 896–7.
Shearer, C. K., McCubbin, F. M., Zeigler, R. A., Gross, J., Simon, S. B., Meshik, A., et al. 2022. Preparing for Artemis Through Lessons Learned from Apollo 17. Highlighting the Progress of the ANGSA Initiative (Abstract #2546). 53rd Lunar and Planetary Science Conference. CD-ROM.
Simon, S. B., Cato, M. J., Shearer, C. K., and the ANGSA Science Team 2022. Results from the 1 mm to 150 μm Fraction of Apollo 17 Drive Tube 73002: Modal Petrology and New Rock Types (Abstract #2211). 53rd Lunar and Planetary Science Conference. CD-ROM.
Simon, S. B., Papike, J. J., and Laul, J. C. 1981. The Lunar Regolith: Comparative Studies of the Apollo and Luna Sites. Petrology of Soils from Apollo 17, Luna 16, 20, and 24 (Abstract). 12th Lunar and Planetary Science Conference, Part B. pp. 371–88.
Smith, M. R., Schmitt, R. A., Warren, P. H., Taylor, G. J., and Keil, K. 1983. Far-Eastern Nonmare Samples: New Data from Luna 20 and 16 (Abstract). 14th Lunar and Planetary Science Conference. p. 716.
Spudis, P. D., and Ryder, G. 1981. Apollo 17 Impact Melts and Their Relation to the Serenitatis Basin. In *Multi-Ring Basins*, edited by P. H. Schultz and R. B. Merrill, 133–48. New York: Pergamon Press. 12th Lunar and Planetary Science Conference, Part A.
Spudis, P. D., Wilhelms, D. E., and Robinson, M. S. 2011. The Sculptured Hills of the Taurus Highlands: Implications for the Relative Age of Serenitatis, Basin Chronologies and the Cratering History of the Moon. *Journal of Geophysical Research* 116: E00H03. https://doi.org/10.1029/2011JE003903.
Stöffler, D., Knöll, H.-D., Marvin, U. B., Simonds, C. H., and Warren, P. H. 1980. Recommended Classification and Nomenclature of Lunar Highlands Rocks—A Committee Report. In *Multi-Ring Basins, Proceedings, Conference on the Lunar Highlands Crust*, edited by J. J. Papike and R. B. Merrill, 51–70. New York: Pergamon Press.
Sun, L., Lucey, P., Flom, A., Ferrari-Wong, C., Zeigler, R. A., Gross, J., Petro, N., Shearer, C., McCubbin, F. M., and the ANGSA Science Team. 2022. Multispectral Imaging of Apollo 17 Core Sample 73002 (Abstract #1890). 53rd Lunar and Planetary Science Conference. CD-ROM.
Swindle, T. D., Spudis, P. D., Taylor, G. J., Korotev, R. L., Nichols, R. H., and Olinger, C. T. 1991. Searching for Crisium Basin Ejecta: Chemistry and Ages of Luna 20 Impact Melts (Abstract). 12th Lunar and Planetary Science Conference, Part B. pp. 167–81.
Taylor, G. J., Drake, M. J., Wood, J. W., and Marvin, U. B. 1973. The Luna 20 Lithic Fragments, and the Composition and Origin of the Lunar Highlands. *Geochimica et Cosmochimica Acta* 37: 1087–106.
Taylor J. 1987. New Samples from Luna 16, 20, and 24. *Lunar News* 49: 4–6. https://curator.jsc.nasa.gov/lunar/lnews/pre2004/ln49.pdf.
Valencia, S. N., Curran, N. M., Bullock, E. S, Corrigan, C. M., and Cohen, B. A. 2022. Quantitative Compositional Mapping of Basalt 73002,186A from the Apollo 17 Station

Three Double Drive Tube (Abstract #2608). 53rd Lunar and Planetary Science Conference. CD-ROM.

Valeniciano, J. L., Neal, C. R., and Shearer, C. K. 2022. An ANGSA Study of Ilmenite Crystal Size Distributions of Basalt Clasts in Drive Tube 73002 (Abstract #2869). 53rd Lunar and Planetary Science Conference. CD-ROM.

Warren, P. H. 1993. A Concise Compilation of Petrologic Information on Possibly Pristine Nonmare Moon Rocks. *American Mineralogist* 78: 360–76.

Welten, K. C., Caffee, M. W., Nishiizumi, K., and the ANGSA Science Team. 2022. Cosmogenic Radionuclides in Lunar Core 73002: Cosmic-Ray Exposure History and Regolith Mixing of the Lunar Surface (Abstract #2389). 53rd Lunar and Planetary Science Conference. CD-ROM.

Wentworth, S., Taylor, G. J., Warner, R. D., Keil, K., Ma, M.-S., and Schmitt, R. A. 1979. The Unique Nature of Apollo 17 VLT Basalts (Abstract). 10th Lunar and Planetary Science Conference. pp. 207–23.

Wieczorek, M., Haskin, L., Korotev, R., Jolliff, B., and Phillips, R. 1998. The Imbrium and Serenitatis Basins: Impacts in an Anomalous Lunar Province. In *Workshop on New Views of the Moon: Integrated Remotely Sensed, Geophysical, and Sample Datasets*, edited by B. L. Jolliff and G. Ryder, 78–9. LPI Contribution 958. Houston, Texas: Lunar and Planetary Institute.

Wilhelms, D. E. 1987. The Geologic History of the Moon. U.S. Geological Survey Professional Paper 1348.

Wolfe, E. W., Bailey, N. G., Lucchitta, B. K., Muehlberger, W. R., Scott, D. H., Sutton, R. L., and Wilshire, H. G. 1981. The Geologic Investigation of the Taurus-Littrow Valley: The Apollo 17 Landing Site. U.S. Geological Survey Professional Paper 1080.

Wolfe, E. W., Lucchitta, B. K., Reed, V. S, Ulrich, G. E., and Sanchez, A. G. 1975. Geology of the Taurus-Littrow Valley Floor. Proceedings, 5th Lunar Science Conference. pp. 2463–82.

Yen, C. J.-K., Jolliff, B. L., Zeigler, R. A., Gross, J., Simon, S. B., Eckley, S. A., Shearer, C. K., and the ANGSA Science Team. 2022. Characterization of Rock Fragment 73002,1017C: An Unusual Lithology Within the Apollo Sample Suite (Abstract #1547). 53rd Lunar and Planetary Science Conference. CD-ROM.

Zeigler, R. A., Gross, J., Eckley, S. A., McCubbin, F. M., and the ANGSA Science Team. 2022. Using X-Ray Computed Tomography to Catalog Rock Fragments in Apollo Drive Tube 73002 (Abstract #2890). 53rd Lunar and Planetary Science Conference. CD-ROM.

SUPPORTING INFORMATION

Additional supporting information may be found in the online version of this article.

Table S1. Results of INAA for samples from the 76001 drive.

Table S2. Results of INAA for samples from Luna 16, 20, and 24.

Table S3. Compositions of model components.

Data S1. Supplementary Information.